Carbohydrate Polymers 92 (2013) 1615–1624

Contents lists available at SciVerse ScienceDirect

Carbohydrate Polymers

journal homepage: www.elsevier.com/locate/carbpol

Heparin-folate-retinoic acid bioconjugates for targeted delivery of hydrophobic photosensitizers

Thanh Huyen Tran[a,1], Byoung-chan Bae[b,1], Yong-kyu Lee[c], Kun Na[b,*], Kang Moo Huh[a,*]

[a] Department of Polymer Science & Engineering, Chungnam National University, 220, Gung-dong, Yuseng-gu, Daejeon 305-764, Republic of Korea
[b] Department of Biotechnology, The Catholic University of Korea, 43-1 Yokkok2-dong, Wonmi-gu, Bucheon City 420-743, Republic of Korea
[c] Department of Chemical and Biological Engineering, Chungju National University, 72, Daehak-ro, Chungju, Chungbuk 380-702, Republic of Korea

ARTICLE INFO

Article history:
Received 12 July 2012
Received in revised form 7 October 2012
Accepted 30 October 2012
Available online 8 November 2012

Keywords:
Heparin bioconjugates
Self-assembled nanoparticles
Encapsulation
Photosensitizer
Targeted delivery

ABSTRACT

Amphiphilic heparin-retinoic acid (HR) and heparin-folate-retinoic acid bioconjugates (HFR) were synthesized by chemical conjugation of a hydrophobic anticancer agent all-trans-retinoic acid (RA) and a targeting ligand, folic acid (FA), to the high molecular weight heparin backbone. The HR and HFR bioconjugates had a high RA content (22%, w/w) and could self-assemble into nanoparticles with efficient encapsulation of a hydrophobic photosensitizer, pheophorbide a (PhA). The HFR bioconjugate demonstrated higher PhA loading content and loading efficiency compared to HR bioconjugate. The PhA-loaded HR and HFR nanoparticles had an average diameter of about 70 nm, a negatively charged surface, a sustained release pattern and self-quenching effect in a buffered solution. Furthermore, the cellular uptake of PhA-loaded HFR nanoparticles in folate receptor-positive HeLa cells was higher than that of PhA-loaded HR nanoparticles. Upon irradiation, HFR nanoparticles selectively enhanced the phototoxicity of PhA in HeLa cells while the dark-toxicity of the nanoparticles was minimal without light treatment. HFR nanoparticles also demonstrated targeted anti-cancer effect, improving the cytotoxicity of RA in HeLa cells compared to HR nanoparticles at RA concentration $\geq$50 μg/mL. The targeting effect of HFR and PhA-loaded HFR nanoparticles was not observed in folate receptor-negative HT-29 cells. The results indicated that HFR nanoparticles may be useful for targeted delivery of hydrophobic PDT agents and as a potential nanocarrier for dual chemo-and photodynamic therapies.

1. Introduction

Photodynamic therapy (PDT) is based on the concept that photosensitizers (PSs), when exposed to light of specific wavelength, generate cytotoxic reactive oxygen species capable of killing tumor cells (Dolmans, Fukumura, & Jain, 2003). Because PSs are typically harmless without light, tumor site treatment can be precisely targeted by selective illumination, limiting damage to surrounding healthy tissues. In addition, PDT has also been shown to damage tumor vasculature through direct effects on vascular endothelial cells (Fingar et al., 1999). However, the clinical application of PDT is limited by the hydrophobic nature and poor tumor selectivity of PSs. Recently, extensive efforts have been devoted to designing various delivery systems for PSs including self-assembled nanoparticles, and polymer/PSs conjugates. In these systems, the aqueous solubility of PSs could be improved by incorporating into the hydrophobic cores of the amphiphilic copolymer or conjugating with hydrophilic polymers (Bae & Na, 2010; Li, Bae, et al., 2011; Li, Moon, et al., 2011). However, there have been few reports on the development of a polymer-drug conjugate for physical entrapment and targeted delivery of a hydrophobic PS.

The self-assembled nanoparticles of amphiphilic polymer-drug conjugates have emerged as one of the most promising nanocarrier systems for various hydrophobic anticancer drugs (Duncan, 2003; Li & Wallace, 2008). The hydrophobic drug rich core can encapsulate another hydrophobic drug for combination therapy while the hydrophilic shell can protect the drug from binding to blood proteins and being absorbed into the reticuloendothelial system, thus keeping the drug in the systemic circulation for a prolonged period of time. Among various biomaterials for preparing the polymer conjugates, heparin, a highly soluble natural polymer, appears as a promising material due to its excellent properties such as high water-solubility, good biocompatibility and surprisingly anti-cancer activities in the processes of tumor progression and metastasis. It was recently suggested that heparin strongly interferes with the activity of growth factors such as basic fibroblast growth factor (bFGF), thereby inhibiting angiogenesis which is essential for tumor progression (Sasisekharan, Shriver, Venkataraman, & Narayanasami, 2002). These distinctive

* Corresponding authors. Tel.: +82 42 821 6663; fax: +82 42 821 8910.
E-mail addresses: kna6997@catholic.ac.kr (K. Na), khuh@cnu.ac.kr (K.M. Huh).
[1] These authors contributed equally to this work.

0144-8617/$ – see front matter © 2012 Elsevier Ltd. All rights reserved.
http://dx.doi.org/10.1016/j.carbpol.2012.10.075

functional activities of heparin have significant advantages in the development of a heparin-based nanoparticulate delivery system.

In the previous study, we have conjugated a low molecular weight heparin with a chemopreventive agent (all-trans-retinoic acid), and a targeting ligand (folic acid). The bioconjugates demonstrated the effective targeting and enhanced cytotoxicity of retinoic acid in folate receptor-positive KB cells (Oh, Cho, Tran, Huh, & Lee, 2012). Despite the advancement in the retinoic acid delivery, the current bioconjugates with low coupling ratio of retinoic acid have limited capacity for physical entrapment of a hydrophobic PS.

The objective of this study is to synthesize a heparin based bioconjugate (HFR) with a higher coupling ratio of retinoic acid by chemical conjugation of high molecular weight heparin with the hydrophobic anticancer drug retinoic acid (RA), an active metabolite of retinol, and the targeting ligand folic acid (FA). This amphiphilic bioconjugate is expected to possess anticancer activity and self-assemble in aqueous media to form nanoparticles that may be useful for encapsulation and targeted delivery of a hydrophobic photosensitizer, pheophorbide a (PhA), for PDT. The hydrophobic pheophorbide a, a second-generation PDT agent, was chosen for this study due to its high singlet oxygen quantum yield of 0.69, high extinction coefficient in the near-infrared region, where tissue penetration of light is maximized (Fernandez, Bilgin, & Grossweiner, 1997), and relatively fast elimination from the body that may shorten side effects caused by long-lasting cutaneous photosensitivity (Hajri et al., 2002).

Physicochemical properties of the PhA-loaded nanoparticles were characterized by various instrumental analyses. The drug release, singlet oxygen quantum yield, cellular uptake behavior and phototoxicity of the PhA-loaded nanoparticles were also evaluated. By conjugating RA and FA to heparin and incorporating PhA into HFR nanoparticles, the nanoparticular system holds great promise as a targeted delivery system for chemotherapy and photodynamic therapy.

2. Materials and methods

2.1. Materials

Unfractionated heparin (UFH, 12,000 Da) was obtained from Mediplex Co. (Korea). All-trans-retinoic acid (RA), folic acid (FA), pyridine, ethylenediamine (EDA), 9,10-dimethylanthracene (DMA), formamide, N,N-dimethyl formamide (DMF), dimethyl sulfoxide (DMSO), N-(3-dimethylaminopropyl)-N′-ethylcarbodiimide hydrochloride (EDC) and N-hydroxysuccinimide (NHS) were purchased form Sigma–Aldrich Chemical Co. (St. Louis, MO, USA). Pheophorbide a (PhA) was purchased from Frontier Scientific Inc. (Logan, UT, USA). N,N′-Dicyclohexylcarbodiimide (DCC) was obtained from Fluka (Buchsm, Switzerland). RPMI 1640 medium and Dulbecco's modified Eagle's medium (DMEM), fetal bovine serum (FBS), antibiotics (penicillin and streptomycin) and Dulbecco's phosphate buffered saline (DPBS) were obtained from GibcoBRL (Invitrogen Corp., Carlsbad, CA, USA). All reagents were analytical grade and used as received without further purification.

2.2. Synthesis of UFH-retinoic acid (HR) and UFH-folic acid-retinoic acid (HFR) bioconjugates

2.2.1. Preparation of aminated RA

The carboxyl group of RA (1 mmol) was activated with EDC (2 mmol) and NHS (2 mmol) in DMF (30 mL) for 6 h, following by the reaction with EDA (10 mmol) at room temperature overnight. After the reaction, unreacted EDA was removed *via* evaporation at 25 °C for 4 h under vacuum. The crude product was precipitated in an excess of cold deionized water and washed several times with deionized water. The aminated RA powder was obtained after lyophilization. The aminated RA was characterized by ^{1}H NMR spectroscopy (JNM-AL400, JEOL Ltd, Japan) at 400 MHz using d_6-DMSO as a solvent.

2.2.2. Preparation of aminated FA

FA (1 mmol) was reacted with DCC (1 mmol) and NHS (2 mmol) in DMSO (20 mL) at room temperature for 12 h. EDA and pyridine (200 μL) were added into the activated FA solution and allowed to react at room temperature overnight. Then, excess acetonitrile was added to the reactant solution for precipitation and removal of DCC and NHS. The aminated FA was obtained after centrifugation and dried under vacuum. The aminated FA was characterized by ^{1}H NMR spectroscopy using d_6-DMSO as a solvent.

2.2.3. Synthesis of HR bioconjugates

HR bioconjugate was synthesized by a coupling reaction of UFH and aminated RA. In brief, UFH (0.01 mmol) was dissolved in formamide (7 mL) by gentle heating, followed by the addition of EDC (0.3 mmol) dissolved in 1 mL formamide. Aminated RA (0.18 mmol) dissolved in DMF (21 mL) was added to the UFH solution and then the mixture was stirred at room temperature for 4 days under nitrogen gas. The crude product was dialyzed against distilled water (MWCO: 2000) for 2 days at room temperature, followed by ultracentrifugation and filtration to remove solvents, EDC and unreacted RA. The yellow product was obtained after lyophilization.

2.2.4. Synthesis of HFR bioconjugates

HFR bioconjugate was synthesized in two steps. Step 1 was the synthesis of UFH-folic acid conjugate (HF): UFH (0.01 mmol) was dissolved in formamide (7 mL) by gentle heating, followed by the addition of EDC (0.2 mmol) dissolved in 1 mL formamide and aminated FA (0.08 mmol) dissolved in formamide. After 2 day reaction at room temperature under nitrogen gas, the product solution was dialyzed (MWCO: 2000) against sodium hydroxide solution (0.1 M) for 1 day and then deionized water for 2 days to remove unreacted EDC, NHS and aminated FA. The final product was obtained as a dark yellow powder after lyophilization. Step 2 was the conjugation of aminated RA with HF: the reaction proceeded for 4 days, followed by the purification procedure as that of HR.

The synthesized HR and HFR bioconjugates were analyzed by ^{1}H NMR spectroscopy as described above.

2.3. Characterization of HR and HFR bioconjugates

The coupling ratios of FA and RA were quantified using a UV–vis spectrophotometer (S-3100, SCINCO, Korea). Briefly, the lyophilized HR and HFR were dissolved in formamide to final concentration of 0.05 mg/mL. The absorbance of FA at 290 nm and of RA at 373 nm was measured using established calibration curves with known concentrations of aminated RA and aminated FA in formamide. The critical aggregation concentrations (CACs) of HR and HFR bioconjugates were analyzed by fluorescence spectrophotometry (FluoroMax-4, Horiba Jobin Yvon), using pyrene as a fluorescence probe (Gao et al., 2008). The pyrene solutions (3×10^{-4} M) in acetone were added into the test tubes, and followed evaporation to remove the organic solvent. Then, various concentrations of HR and HFR solutions (10 mL) were added to the test tubes and sonicated for 3 h at 60 °C to equilibrate the pyrene and the nanoparticles. The concentration of sample solution was varied from 0.005 to 0.5 mg/mL. The final concentration of pyrene was 6.0×10^{-7} M. The emission spectra of pyrene were recorded in the range of 350–450 nm at the excitation wavelength of 336 nm. For the measurement of the intensity ratio of the first, (374.5 nm) and the third

highest energy bands (386 nm) in the pyrene emission spectra the slit opening was set at 2.5 nm (emission).

2.4. Preparation and characterization of PhA-loaded HR and HFR nanoparticles

PhA-loaded nanoparticles were prepared by a dialysis method. Briefly, HR or HFR bioconjugates (20 mg) were dissolved in formamide (10 mL), followed by the addition of 4 mg PhA (20%, w/w) dissolved in formamide (2 mL). The mixture was then dialyzed against distilled water for 2 days (MWCO: 2000). The precipitated PhA was removed by centrifugation at 10,000 rpm for 15 min, followed by the filtration through 0.45 μm syringe. The final products were obtained after lyophilization. The average particle size, size distribution and zeta-potential of the PhA-loaded nanoparticles were measured using a dynamic light scattering (DLS) instrument (ELS-Z series, Otsuka Electronics, Japan). The morphologies of HR and HFR nanoparticles were imaged by scanning electronic microscopy (SEM) (JSM-6700, Japan) at 10 kV. Specimens were prepared by dropping a solution of HR or HFR nanoparticles to the surface of a silicon wafer, followed by drying under vacuum. The samples for particle size and SEM measurements were prepared by dispersion of 5 mg lyophilized PhA-loaded nanoparticles into 5 mL of deionized water, followed by sonication for 10 min and filtration through a 0.45 μm syringe filter.

The amount of PhA-loaded into HR and HFR nanoparticles was determined by a colorimetric method. The lyophilized PhA-loaded HR and HFR nanoparticles were dissolved in 10 mL formamide to obtain clear solutions. The absorbance at 669 nm was detected with a UV–vis spectrophotometer. PhA solutions were prepared at various concentrations and the absorbance at 669 nm was measured to generate the calibration curve for calculating the drug-loading content. The drug-loading content (DLC) and encapsulation efficiency (EE) were calculated by the following equations:

$$\mathrm{DLC} = \frac{\text{Amount of PhA in nanoparticles}}{\text{Amount of PhA-loaded nanoparticles}} \times 100$$

$$\mathrm{EE} = \frac{\text{Amount of PhA in nanoparticles}}{\text{Amount of PhA used for nanoparticle preparation}} \times 100$$

2.5. In vitro release of PhA from HR and HFR nanoparticles

In vitro release of PhA from HR and HFR nanoparticles was studied using a dialysis technique. Briefly, lyophilized PhA-loaded HR and HFR nanoparticles (4 mg) were suspended in 2 mL of PBS (0.01 M, pH 7.4) under gentle heating, followed by sonication for 10 min to give an optically clear solution. The solutions were introduced into dialysis bags (MWCO: 2000) and immersed in 20 mL of PBS at 37 °C in a shaking bath at 100 rpm. At selected time intervals, aliquots (3 mL) were removed from the dissolution medium and an equivalent volume of fresh PBS was compensated. The aliquots were lyophilized, followed by mixing with 2 mL of methanol. The absorbance was read by a UV–vis spectrophotometer at 669 nm. The amount of PhA released was calculated by comparing with standard.

2.6. Determination of singlet oxygen generation

The generation of singlet oxygen can be measured by the decrease of fluorescence intensity of 9,10-dimethylanthracene (DMA) utilizing fluorescence spectroscopy. A standard stock solution of DMA in DMF was stored at 4 °C in the dark until it was used, at which time it was diluted to a final concentration of 1.184×10^{-5} M with DMF or PBS buffer. PhA-loaded HR and HFR nanoparticles were also dissolved in DMF or dispersed in PBS buffer (pH 7.4) at 5 μg/mL PhA equivalence and then added to DMA stock solutions to give a final concentration of 20 μM DMA. The mixtures were irradiated at a light intensity of 7 mW/cm^2 using a 670 nm laser source (Institute of Electronics). A collimated laser beam was directed at the sample cuvette through an optical fiber. The decrease in fluorescence intensity of DMA (emission 380–550 nm, with excitation at 360 nm) as a result of singlet oxygen generation was monitored using a spectrofluorophotometer controlled by a PC. Singlet oxygen quantum yield (SOQ) was calculated by the following equation (Hoebeke & Damoiseau, 2002):

$$\Phi_\Delta = \frac{k_S}{k_R} \times \frac{A_R}{A_S} \times \mathrm{ref}.\Phi_\Delta$$

where A is absorbance at 670 nm (the excitation wavelength), k is the gradient of the absorbance curve, S refers to the sample and R to the reference. SOQ (Φ_Δ) of each sample was calculated from the reference Φ_Δ value (PhA 0.52: ref. Φ_Δ) (Fernandez et al., 1997; Roslaniec, Weitman, Freeman, Mazur, & Ehrenberg, 2000).

2.7. Cytotoxicity of PhA-loaded HR and HFR nanoparticles

HeLa cells (folate receptor-positive, 5×10^4 per well) and HT-29 cells (folate receptor-negative, 5×10^4 per well) were seeded on 96-well plates and cultured in completely lightproof plates containing 200 μL of culture medium for 24 h. After incubation for 12 h with different concentrations of PhA-loaded HR, PhA-loaded HFR nanoparticles and free PhA (0.01–2 μg/mL of PhA equivalence), the medium was replaced with fresh RPMI 1640 just prior to irradiation at 1.2 J/cm^2 by a 670 nm laser source (Institute of Electronics). The nanoparticle solutions for the cytotoxicity assay were prepared by dispersing the freeze-dried nanoparticles in the serum free media. However, free PhA is a hydrophobic photosensitizer. Thus the drug solution was prepared by dissolving PhA in DMSO at 1 mg/mL concentration and then diluting with the serum free media. After 24 h of incubation, phototoxicity and dark-toxicity were determined using 3-[4,5-dimethylthiazol-2-yl]-3,5-diphenyltetrazolium bromide dye (MTT dye, 2 mg/mL) uptake at 570 nm on an ELISA reader. To measure the cytotoxicity of HR and HFR, HeLa and HT-29 cell lines were incubated with HR and HFR at different RA equivalences (12.5–100 μg/mL) for 24 h and then the cell viability was determined using MTT assay.

2.8. Intracellular uptake of PhA-loaded HR and HFR nanoparticles

HeLa cells and HT-29 cells were grown from a density of 5.0×10^5 cells/well on 6-well plate at 37 °C in a humidified atmosphere of 5% CO_2 for 24 h. Serum-free RPMI 1640 containing PhA-loaded HR, HFR and free PhA at 0.5 μg/mL PhA was added and cells were incubated for 6 h. Cells were then washed three times, harvested with DPBS and transferred into FACS tubes. All samples were analyzed by a FACScan flow cytometer (Beckman, San Jose, CA, USA) to determine cellular internalization. Fluorescence measurement of intracellular PhA was done in the FL4 channel with the emission at 670 nm.

To observe cellular uptake, HeLa cells and HT-29 cells were seeded at a density of 1.0×10^5 cells/well on 18 mm × 18 mm sterile cover glasses inserted into 12-well plates and preincubated for 24 h. Serum-free RPMI 1640 containing PhA-loaded HR, HFR and free PhA at 0.5 μg/mL PhA was added to each well, followed by the incubation for 6 h at 37 °C. The cells were then rinsed with DPBS, and fixed with 4% paraformaldehyde solution for 10 min. Cover glasses were then placed on the slide glasses. Cellular uptake of free PhA, PhA-loaded HR and HFR nanoparticles was monitored by fluorescence microscopy (Olympus, USA).

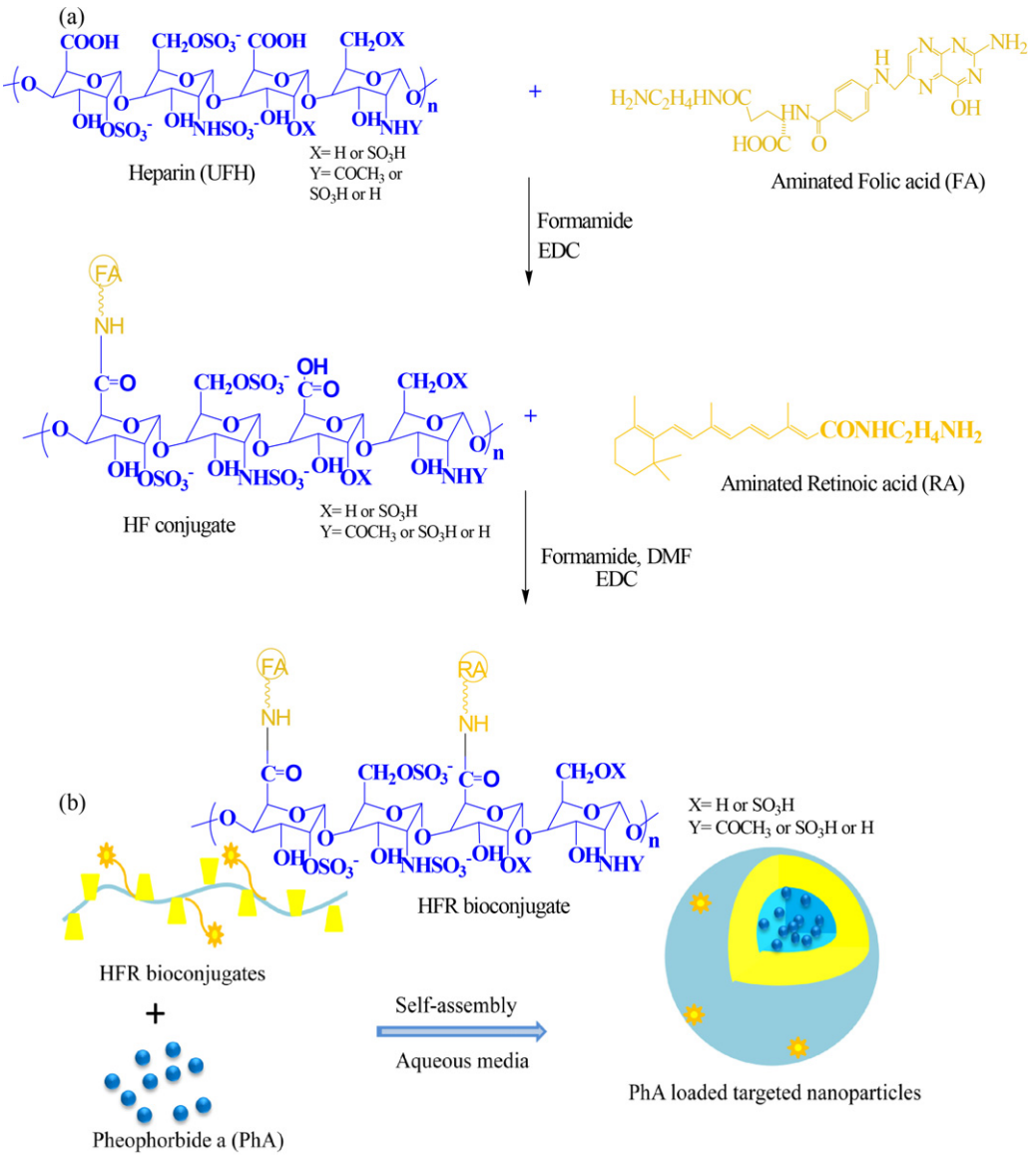

Scheme 1. (a) Synthetic route of HFR bioconjugates from UFH, FA and RA; (b) schematic illustration of PhA loading into HFR nanoparticles.

3. Results and discussion

3.1. Synthesis and characterization of nanoparticles

We synthesized amphiphilic HR and HFR bioconjugates and investigated their ability for encapsulation and targeted delivery of PhA for photodynamic therapy. The HF conjugate was initially prepared by a coupling reaction between the carboxyl groups of UFH with the amine groups of aminated FA. The carboxyl groups of HF conjugate was then reacted with amine group of aminated RA to produce HFR bioconjugate (Scheme 1a). HR bioconjugate was synthesized by the reaction of UFH with aminated RA. Reaction yield was about 70% for both HR and HFR bioconjugates. The chemical composition of HR and HFR bioconjugates was confirmed by ^{1}H NMR measurement (Fig. 1). The characteristic chemical shifts of UFH were observed at 1.8, 3.1, 3.6 and 4.0 ppm. The proton assignments of aminated RA were given at 1.0, 1.2, 1.4, 2.3–2.8 and 6.2–6.4 ppm. The ^{1}H NMR spectra of HR and HFR compromised all characteristic peaks of both UFH and RA and new amide linkages between UFH and RA appeared at 7.96 ppm, indicating the successful conjugation of RA to UFH. The presence of FA molecule in HFR bioconjugate was confirmed by the appearance of weak signals at 6.7–8.5 in the ^{1}H NMR spectrum of HFR, which corresponded to the aromatic protons of FA (Wang, Wang, Xiang, & Yao, 2010). The coupling ratio of RA in HR and HFR was about 11, corresponding to 22% (w/w) RA content, and the coupling ratio of FA in HFR was 2 (Table 1), corresponding to RA and FA feed molar ratios of 18 and 5, respectively. The CAC value of HFR bioconjugate was lower than that of HR bioconjugate, showing the values of 23 and 79 mg/L, respectively, indicating that HFR bioconjugate was more stable than HR bioconjugate. These CAC values were in the typical range of polymer-drug conjugates (Bae & Na, 2010; Hou et al., 2011) suggesting that the heparin based bioconjugates may circulate as self-assembled nanoparticles *in vivo* for an extended period of time. The aqueous solutions of the nanoparticles stored at room temperature (25 °C) were stable for at least 6 months without any detectable aggregation (data not shown).

3.2. Preparation and characterization of HFR and PhA-loaded HFR nanoparticles

The HR and HFR bioconjugates readily self-assembled upon contact with aqueous media to form nanoparticles. The driving force of their self-assembling behavior is the hydrophobic interaction

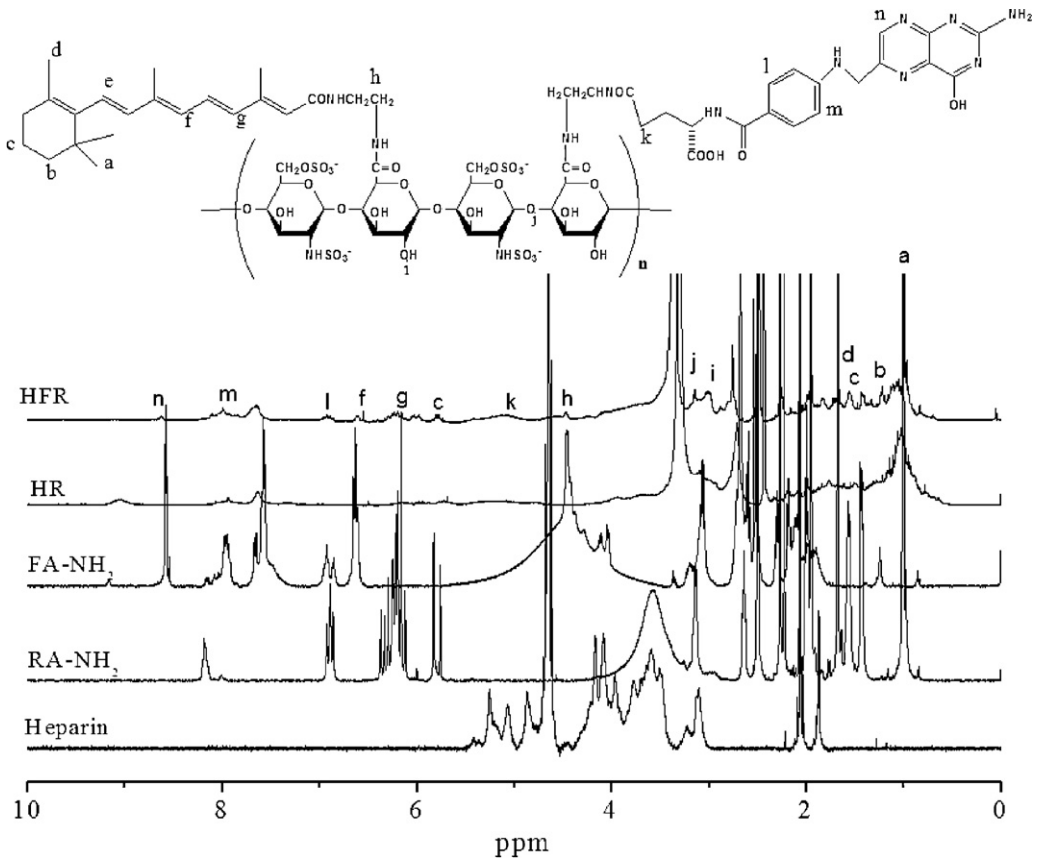

Fig. 1. ^{1}H NMR spectra of UFH in D_2O, RA-NH_2, FA-NH_2, HR and HFR in d_6-DMSO.

between conjugated RA moieties. The HR and HFR self-assembled nanoparticles likely have a core/shell structure bearing a hydrophobic RA inner core that could served as a container for hydrophobic drugs. The hydrophobic PhA was successfully encapsulated into HR and HFR nanoparticles by a dialysis method (Scheme 1b). At lower coupling ratio of RA such as 2 or 4, the HFR and HR bioconjugates had limited capacity for the encapsulation of PhA (data not shown). With the PhA feed ratio of 20% (w/w), the DLC in HR nanoparticles was about 8.7% with EE of 33%. Despite similar RA coupling ratio, HFR nanoparticles showed about two-fold higher DLC (15.6%) and 2.5-fold higher EE (82%) compared to HR nanoparticles (Table 1). The results indicated that the presence of folic acid enhanced the encapsulation of PhA into the core of HFR nanoparticles. This could be attributed to the hydrophobic nature of folic acid favoring PhA encapsulation.

The particle size and morphology of self-assembled HR, HFR and PhA-loaded nanoparticles were measured by DLS and SEM, respectively. The average particle size of HR and HFR nanoparticles was 155 and 139 nm, respectively (Table 1), indicating that the conjugation of folate ligand decreased the size of HR nanoparticles. The smaller size of the folate-conjugated nanoparticles indicates that the FA favors the formation of more compact structures with respect to the non-folate-conjugated nanoparticles (Scomparin, Salmaso, Bersani, Fainaro, & Caliceti, 2011). After PhA loading, the average particle size of PhA-loaded HR and PhA-loaded HFR nanoparticles remarkably decreased to 65 and 69 nm, respectively. The result indicated that the encapsulated PhA endows increased hydrophobicity, resulting in the formation of dense nanoparticle structure. This decrease of particle size of PhA-loaded HR and HFR nanoparticles is in good agreement with the behavior of glycol chitosan-N-acetyl histidin nanoparticles whose particle size was decreased after encapsulation of hydrophobic doxorubicin (Lee et al., 2010). The SEM images showed that the nanoparticles with and without PhA loading were almost spherical in shape with sizes of 60–100 nm for HR and PhA-loaded HR, and smaller sizes of 50–80 nm for HFR and PhA-loaded HFR nanoparticles (Fig. 2). The

Table 1
Characterization of HR, HFR conjugates and pheophorbide a (PhA)-loaded nanoparticles (HR-P and HFR-P).

Samples	Coupling ratio[a]	CAC (mg/L)	PhA feed ratio (%, w/w)	DLC (%)	EE (%)	Average size (nm)	PDI	Zeta potential (mV)	SOQ[b]	
									DMF	PBS
HR	1:11.21	79				155.4 ± 0.9	0.15 ± 0.05	−35.5 ± 0.8		
HFR	1:2.2:10.96	23				139.1 ± 2.9	0.17 ± 0.03	−30.1 ± 0.7		
HR-P			20	8.6 ± 0.4	33.0 ± 1.2	65.4 ± 9.1	0.05 ± 0.01	−33.8 ± 1.4	0.33	0.15
HFR-P			20	15.7 ± 0.7	82.2 ± 1.7	69.7 ± 1.6	0.06 ± 0.02	−28.5 ± 0.8	0.40	0.07

[a] H:RA and H:FA:RA.
DLC: drug loading content.
EE: encapsulation efficiency.
[b] SOQ of PhA in DMF and PBS is 0.52 and 0.31, respectively.

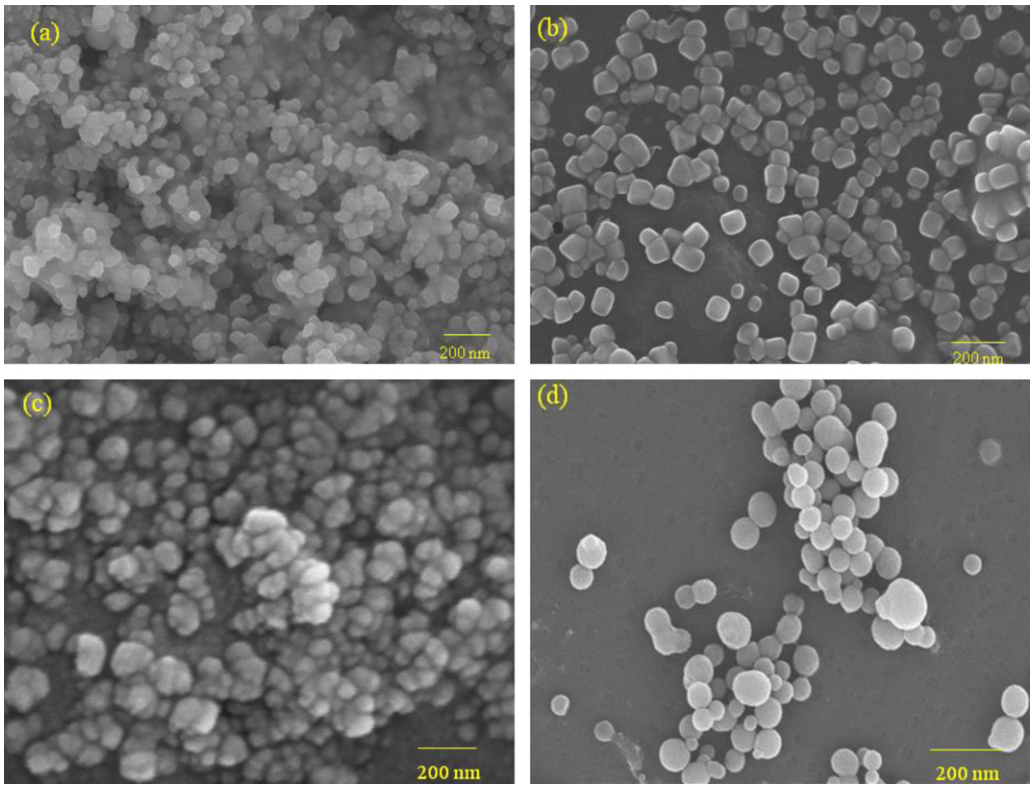

Fig. 2. SEM images of (a) HR, (b) PhA-loaded HR, (c) HFR and (d) PhA-loaded HFR nanoparticles.

ideal size for self-assembled nanoparticles to achieve passive tumor targeting *via* an enhanced permeation and retention (EPR) effect is less than 200 nm (Cho, Wang, Nie, Chen, & Shin, 2008). Therefore, the nano-scaled particle size (<100 nm) of the PhA-loaded HR and HFR nanoparticles would be favorable for passive tumor targeting *via* the EPR effect. The HR and HFR nanoparticles were negatively charged at their surface, as reflected in the zeta-potential values of −35.5 and −30 mV, respectively (Table 1), indicating that negatively charged UFH covers the self-assembled nanoparticles. HFR nanoparticles showed slightly less negative charge than HR nanoparticles, which was consistent with consumption of UFH carboxyl groups by the coupling with FA molecules. After PhA loading, HR and HFR nanoparticles retained negative zeta potentials, which could increase their long-term stability in the systemic circulation.

3.3. Drug release profiles and singlet oxygen quantum yield of PhA-loaded nanoparticles

To assess the potential of PhA-loaded HR and HFR as nanoscale drug carriers, we performed PhA release test in PBS (pH 7.4, 37 °C). Both HR and HFR nanoparticles released PhA in a sustained release pattern for 3 weeks without initial burst release, showing the value of about 5% for HFR and 11% for HR after the first day, and about 50% for HFR and 70% for HR nanoparticles after 3 weeks (Fig. 3). The sustained release of PhA from the nanoparticles may be due to diffusion of incorporated PhA molecules that interacted strongly with the hydrophobic cores of the nanoparticles (Li, Moon, et al., 2011; Lee et al., 2009). The PhA release from HR nanoparticles was significantly faster than that from HFR nanoparticles at all points, probably due to lower DLC leading to the faster diffusion pathway.

Generation of singlet oxygen, which governs the phototoxicity of the PhA-loaded nanoparticles, was determined by measuring the decrease of fluorescence intensity of DMA as the $^1O_2$ trap. Faster decrease of DMA fluorescence intensity indicates faster generation of singlet oxygen. When we irradiated free PhA and PhA-loaded nanoparticles dissolved in DMF with light, DMA fluorescent intensity decreased rapidly, showing the remaining percent of 37%, 48% and 56% for free PhA, PhA-loaded HFR and PhA-loaded HR nanoparticles after 4 min, respectively (Fig. 4a). This result indicated rapid generation of singlet oxygen as a function of the time of light exposure when free PhA, PhA-loaded HR and PhA-loaded HFR nanoparticles were dissolved in DMF. However, decrease in DMA fluorescent intensity was slower when PhA-loaded nanoparticles dissolved in PBS, showing values of 60%, 70% and 72% for free PhA, PhA-loaded HR and PhA-loaded HFR nanoparticles after 4 min, respectively, indicating that the generation of singlet oxygen significantly decreased in PBS (Fig. 4b). Singlet oxygen quantum yields (Φ_Δ) of PhA-loaded HR and PhA-loaded HFR in DMF were calculated as 0.33 and 0.40, respectively, by a comparison of the

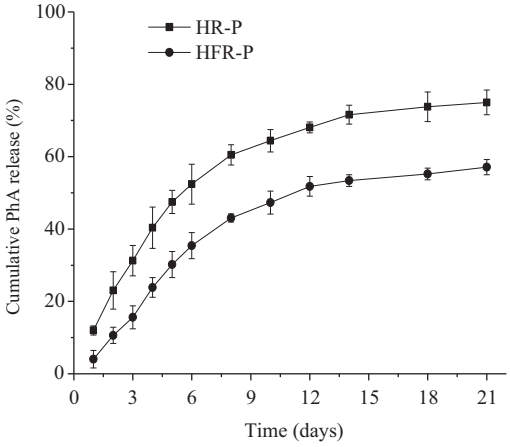

Fig. 3. PhA release profiles of PhA-loaded HR and HFR nanoparticles in PBS buffer (pH 7.4).

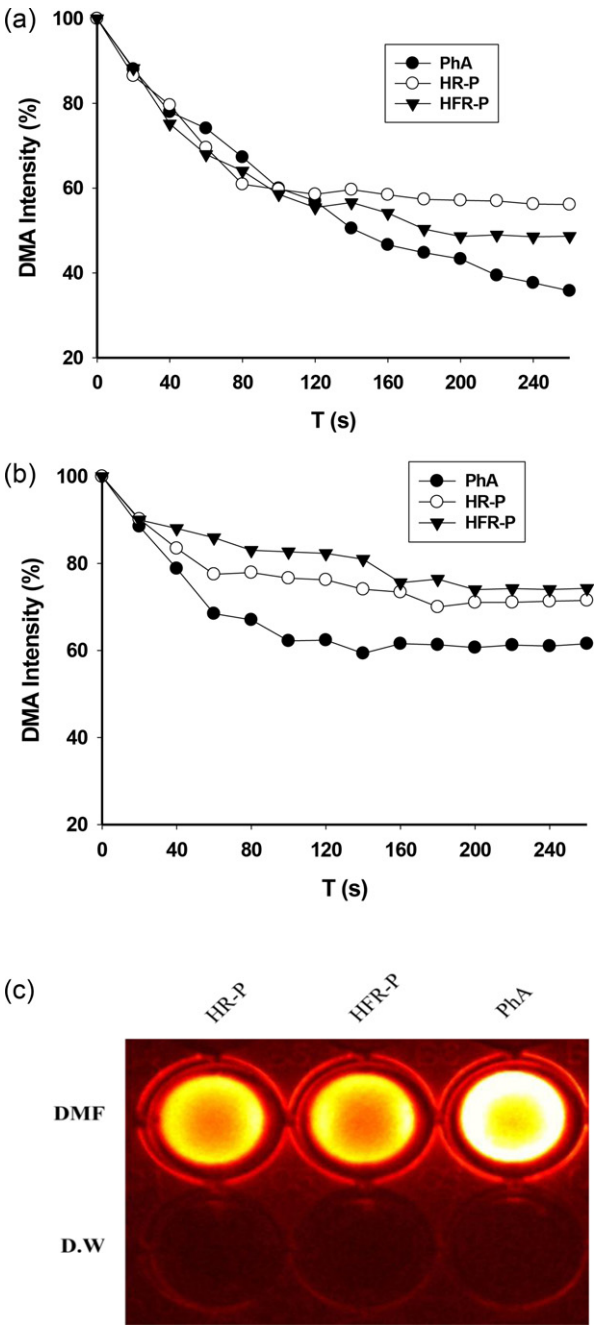

Fig. 4. Change in 9,10-dimethylanthracene (DMA) fluorescence due to generation of singlet oxygen generation after irradiation of free PhA and PhA-loaded nanoparticles in (a) DMF, (b) PBS and (c) NIRF images of free PhA and PhA-loaded nanoparticles in DMF and PBS at 5 μg/mL PhA.

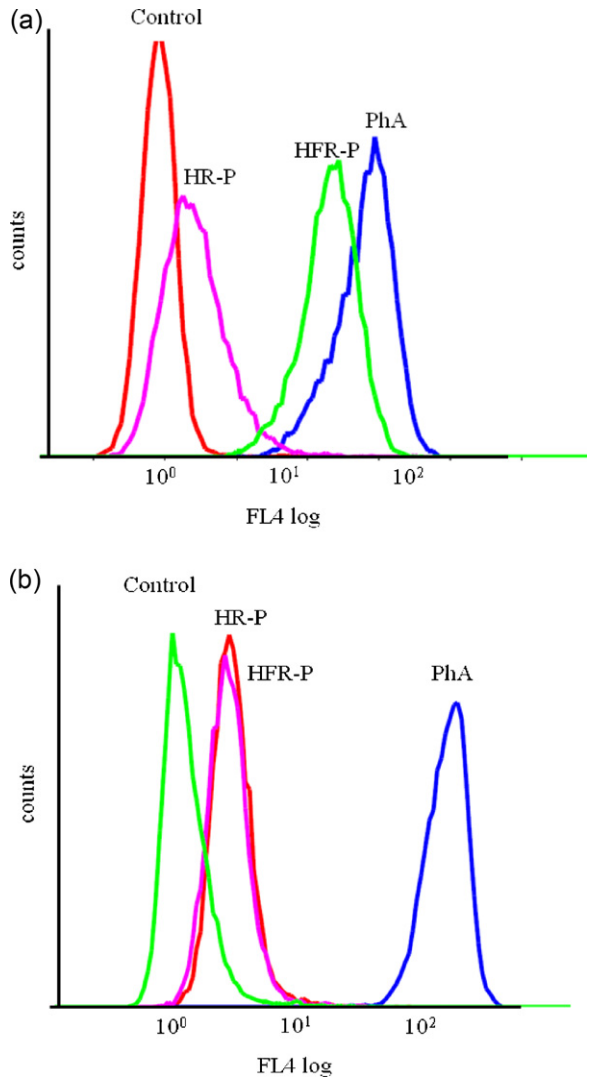

Fig. 5. Fluorescent intensity analyzed by fluorescence activated cell sorting (FACS) of (a) HeLa cells and (b) HT-29 cells after 6 h incubation at 37 °C with free PhA and PhA-loaded nanoparticles at 0.5 μg/mL PhA.

slope for PhA-loaded HR and HFR nanoparticles with the corresponding slope for free PhA ($\Phi = 0.52$) (Table 1). However, the Φ_{Δ} value of PhA-loaded HR and HFR nanoparticles dramatically decreased in PBS, showing the value of 0.15 and 0.07, respectively, indicating the self-quenching effect of PhA inside the nanoparticles. The lower SOQ value of PhA-loaded HFR than PhA-loaded HR nanoparticles indicated higher self-quenching effect of PhA, probably due to stronger interaction of more encapsulated PhA in the higher DLC of HFR compared to HR nanoparticles. To further confirm the self-quenching effect, Fig. 4c shows near-infrared fluorescence (NIRF) images of free PhA and PhA-loaded nanoparticles in DMF or PBS. Due to the FRET effect induced by the encapsulated PhA *via* hydrophobic and π–π stacking interactions (Li, Bae, et al., 2011), the NIRF emissions of free PhA, PhA-loaded HR and HFR nanoparticles were obscure in lipophobic (PBS) solvent. Contrasting NIRF images were observed when free PhA, PhA-loaded HR and HFR nanoparticles were dissolved in lipophilic (DMF) solvent. Based on these results, we assumed that PhA molecules could be encapsulated in the HFR nanoparticles, but some of aggregated PhA at the inner core may form self-quenched aggregates. The reduced singlet oxygen quantum yield characteristics of PhA-loaded HFR nanoparticles in aqueous media is in good agreement with other PS nanoparticle systems such as pullulan/folate-PS conjugates, PS-loaded glycol chitosan-cholanic acid conjugates (Bae & Na, 2010; Lee et al., 2009). However, compared to HA or glycol chitosan-based systems, heparin-based delivery systems have the further advantage of antiangiogenic effect of heparin, and thereby inhibition of tumor progression (Sasisekharan et al., 2002). Furthermore, the HFR and HR nanoparticles may have the anti-cancer effect of RA by binding to retinoic acid receptors present on the nuclear membrane of cancer cells to induce growth inhibition, differentiation or apoptosis (Li, Qi, Maitani, & Nagai, 2009). Thus, chemotherapy and PDT effects might be achieved from HFR nanoparticles by controlling the dose of the anticancer drug and photosensitizer, and the dose of light treatment for PDT.

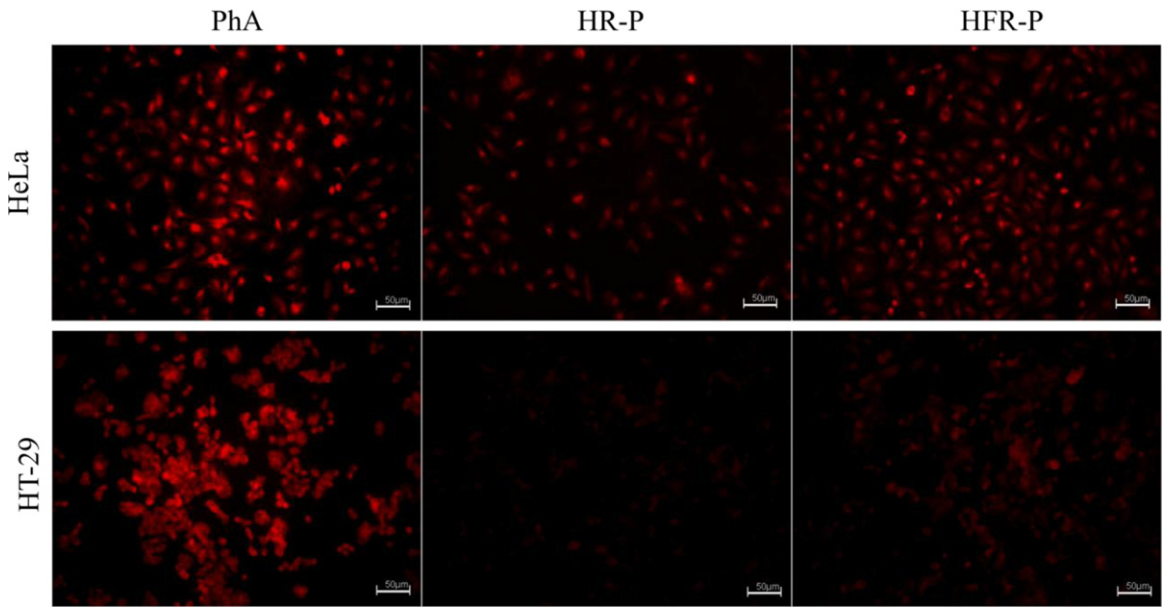

Fig. 6. Fluorescence microscopy images of HeLa and HT-29 cells treated with PhA, PhA-loaded HR and HFR nanoparticles for 6 h at the same concentration of PhA. Scale bars are 50 μm.

The self-quenching effect of the PS-loaded nanoparticles in an aqueous medium is advantageous for lowering the side effects of PDT, such as skin photosensitivity. During the circulation, the phototoxicity of PS can be suppressed until it reaches the target site, where the suppression can be rapidly reversed by the dissociation and degradation of the nanoparticles *via* enzymatic activity (Bae & Na, 2010; Li, Bae, et al., 2011).

3.4. Cellular uptake of PhA-loaded nanoparticles

To evaluate the cellular uptake behavior of the PhA-loaded nanoparticles, we used HeLa as folate receptor-positive tumor cells and HT-29 as folate receptor-negative tumor cells. Fig. 5 shows flow cytometry profiles of HeLa and HT-29 cells incubated for 6 h with free PhA, PhA-loaded HR and PhA-loaded HFR nanoparticles. Cells without any PhA treatment were used as a negative control. With the equivalent PhA concentration in each formulation (0.5 μg/mL PhA) and the same incubation time, PhA-loaded HFR displayed a higher fluorescence intensity in HeLa cells than PhA-loaded HR showing a right shift of the fluorescence peak compared to negative control (Fig. 5a), indicating that the folate-conjugation enhanced the uptake of the PhA-loaded nanoparticles in folate receptor-positive cells. The fluorescence peaks overlapped in HT-29 cells treated with PhA-loaded HR and PhA-loaded HFR nanoparticles, indicating the similar uptake of the nanoparticles in HT-29 cells due to the lack of folate receptors (Fig. 5b). In both HeLa and HT-29 cell lines, the fluorescence intensity of free PhA was significantly greater than that of PhA-loaded HR and PhA-loaded HFR nanoparticles, indicating higher cellular uptake of free PhA compared to the PhA-loaded nanoparticles which could be attributed to the faster diffusion of small molecules than nanoparticles into cells (Guo et al., 2011). Therefore, free PhA cannot be used in a targeted cancer therapy due to its non-specific property.

Cellular uptake of free PhA, PhA-loaded HR and PhA-loaded HFR nanoparticles was also visualized by fluorescence microscopy as shown in Fig. 6. HeLa cells treated with free PhA and PhA-loaded HFR nanoparticles showed high intensity of red fluorescence signal originating from PhA, indicating the efficient internalization of free PhA and PhA-loaded HFR nanoparticles into HeLa cells. However, HeLa cells incubated with PhA-loaded HR nanoparticles displayed weaker fluorescent signals, indicating a lower degree of internalization compared to PhA-loaded HFR nanoparticles. On the other hand, the red emission intensity of PhA from these nanoparticles was similar in HT-29 cells and significantly weaker than that in HeLa cells. The results indicated greater uptake of PhA-loaded HFR nanoparticles compared to PhA-loaded HR nanoparticles, which was in accordance with the flow cytometry results.

It is known that non-targeted nanoparticles are taken up *via* non-specific endocytosis mechanism while the uptake of targeted nanoparticles occurs through specific endocytosis process. The rate of the specific endocytosis was much faster than that of the non-specific one (Guo et al., 2011). Thus, the better cellular uptake of the HFR nanoparticles compared to the HR nanoparticles putatively results from a specific interaction between FA on the HFR and folate receptors on the HeLa cells. It is well known that nanoparticles with ideal size are accumulated within the tumor microenvironment by EPR effect. However, accumulation within tumor microenvironment by the EPR effect may not always correlate with therapeutic outcome, since cellular internalization is required for anticancer drugs to exert their biological function inside tumor cells (Wang et al., 2009). The results suggest that the enhanced cellular uptake of PhA-loaded HFR nanoparticles may improve the therapeutic effect of both RA and PhA in the folate receptor-positive tumor cells.

3.5. In vitro cytotoxicity of HFR and phototoxicity of PhA-loaded HFR nanoparticles

To investigate the photocytotoxicity of PhA-loaded HFR nanoparticles, we measured the viability of cancer cells treated with free PhA and the PhA-loaded nanoparticles with or without light treatment using MTT cytotoxicity assay. Fig. 7 showed the viability of HeLa and HT-29 cells treated with free PhA and the PhA-loaded nanoparticles at different equivalent PhA concentrations without or with light treatment at dose of 1.2 J/cm^2 at 670 nm. In HeLa cells with light treatment, free PhA and PhA-loaded nanoparticles dose dependently (0.1–2 μg/mL PhA) decreased cell viability by 20–87% (Fig. 7a), implying that the PhA containing nanoparticles effectively generated the cytotoxic species and induced the cell depletion. At similar PhA level, the cytotoxicity of PhA-loaded HFR nanoparticles was significantly higher than that of PhA-loaded

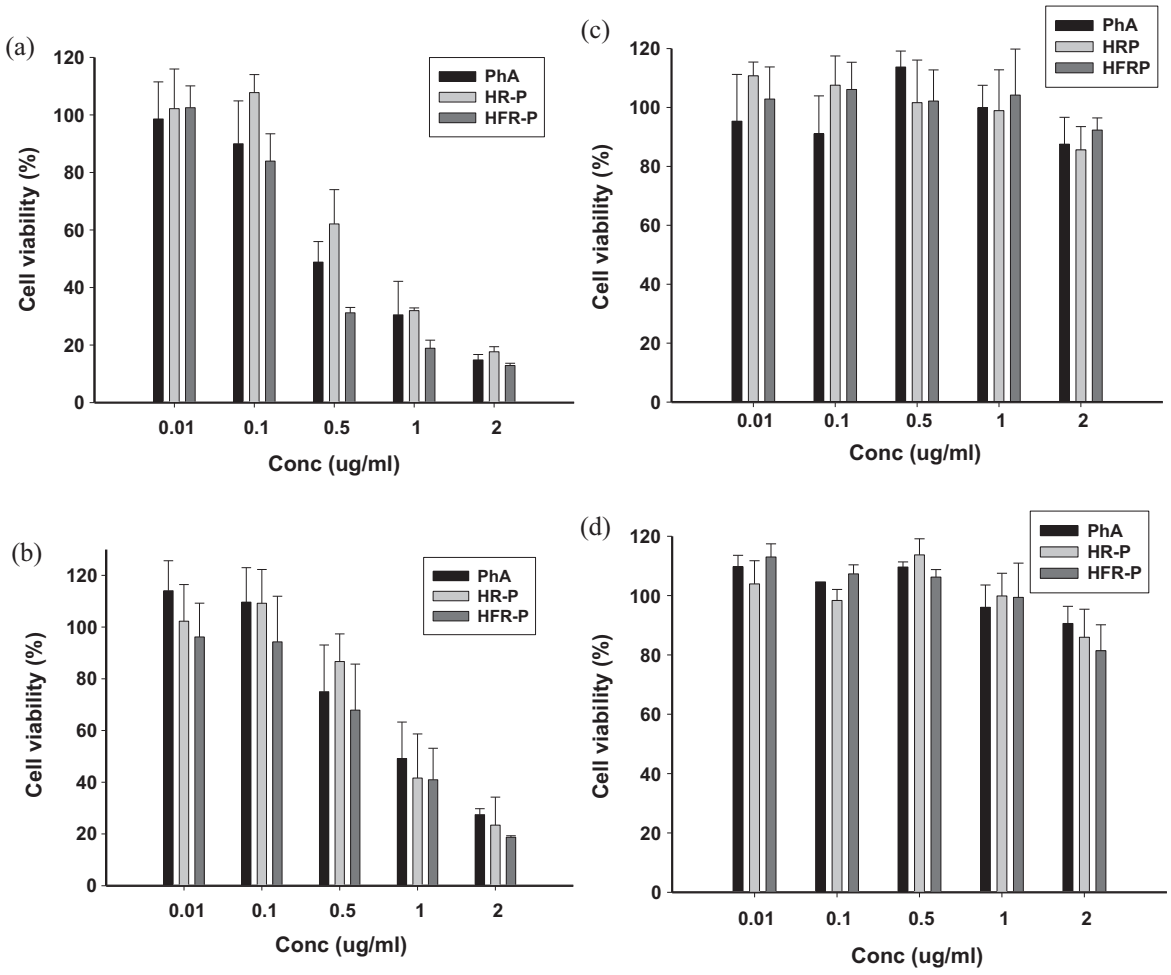

Fig. 7. Phototoxicity of free PhA and PhA-loaded nanoparticles in (a) HeLa cells, (b) HT-29 cells and dark-toxicity of free PhA and PhA-loaded nanoparticles in (c) HeLa cells, (d) HT-29 cells at different equivalent concentrations of PhA.

HR nanoparticles, giving cell viability values of 30% and 60% at 0.5 μg/mL PhA, respectively, indicating that the targeting effect of FA conjugated nanoparticles could further enhance the therapeutic effects. However, the targeting effect of FA was negligible at high concentration of PhA (2 μg/mL), putatively due to the similar uptake of PhA into HeLa cells at saturated PhA concentration. In HT-29 cells with light treatment, the cytotoxicities of PhA-loaded HFR nanoparticles and PhA-loaded HR nanoparticles were insignificantly different at similar PhA concentrations in the range of 0.01–2 μg/mL due to the similar uptake of the nanoparticles in the folate receptor-negative HT-29 cells (Fig. 7b). The presence of a selected targeting moiety and its content in a polymer-anticancer drug conjugate can be relevant in determining cancer targeting and selective cytotoxicity. The loss of activity with the increase of FA moieties per polymer chain due to steric entanglement and aggregation effects of the conjugates has been reported (Canal, Vicent, Pasut, & Schiavon, 2010). The results of cellular uptake and cytotoxicity indicated that a 2.0 coupling ratio of FA to the UFH backbone was suitable for targeting effect of HFR nanoparticles.

Without light treatment, the viability of both HeLa and HT-29 cells treated with free PhA and PhA-loaded nanoparticles was in the range of 81-110% even at high concentration of PhA (2 μg/mL) (Fig. 7c and d). The results indicated that PhA-loaded HR and HFR nanoparticles not only have remarkable phototoxicity but also are minimally toxic to the cell lines in the absence of light. To investigate contribution of RA to the cytotoxicity of PhA-loaded HFR nanoparticles without light treatment, we measured the viability of HeLa and HT-29 cells treated with HR and HFR nanoparticles at different equivalent RA concentrations. The HR and HFR nanoparticles did not induce cytotoxicity at RA concentration up to 50 μg/mL in HT-29 cell and 25 μg/mL in HeLa cells (Fig. 8). At these concentrations of RA, the concentration of the nanoparticles was significantly higher than the nanoparticle concentration used for phototoxicity tests. Thus, the contribution of RA toxicity is minimal to the phototoxicity of PhA-loaded HR and PhA-loaded HFR nanoparticles at the tested PhA concentrations. However, the HFR nanoparticles may be useful for combined chemo- and photodynamic therapies by increasing the dose of Pheo-loaded HFR and reducing the light dose. The HR and HFR nanoparticles had significant cytotoxicity in both HeLa and HT-29 cells at higher RA concentration (100 μg/mL), with cell viabilities ranging from 20 to 50%. Furthermore, at the same RA concentration (50–100 μg/mL), HFR showed higher cytotoxicity in HeLa cells compared to HR while the cytotoxicity of these nanoparticles was insignificantly different in HT-29 cells, indicating targeted anti-cancer effect of folate conjugated nanoparticles. Taken together, the PhA-loaded nanoparticles showed both remarkable PDT and targeting effect while the HFR nanoparticles showed targeted anti-cancer effect at higher nanoparticle concentration even without light treatment. Therefore, the HFR nanoparticles could be a potential carrier for the targeted delivery of both RA and PhA with minimal side effects.

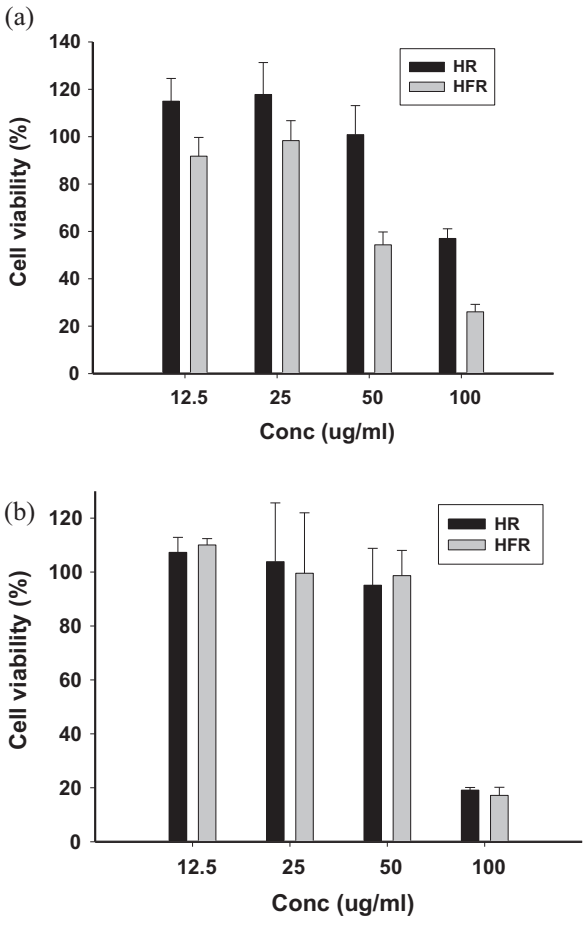

Fig. 8. Cell viability of (a) HeLa cells, (b) HT-29 cells after treatment with HR and HFR nanoparticles at different equivalent concentrations of RA for 24 h.

4. Conclusion

In this study, amphiphilic heparin-folate-retinoic acid bioconjugate (HFR) was synthesized and characterized. Hydrophobic pheophorbide a (PhA) was successfully encapsulated into the HFR nanoparticles by a dialysis method. The HFR nanoparticles had higher PhA loading content and encapsulation efficiency than the nanoparticles without folate. PhA-loaded HFR nanoparticles displayed a self-quenching effect in PBS, while the generation of singlet oxygen significantly increased in DMF. The nanoscale size, negatively charged surface and long-term release profiles of PhA-loaded HFR nanoparticles could enable them to serve a passive targeting system. Furthermore, the presence of folate targeting molecules could efficiently enhance the cellular uptake and *in vitro* phototoxicity of PhA-loaded HFR nanoparticles in folate receptor-positive HeLa cells with light treatment. The phototoxicity and targeting effect of these nanoparticles were minimal without light treatment at the tested PhA concentrations. At RA concentration higher than 50 μg/mL, HFR nanoparticles induced significantly higher cytotoxicity than HR nanoparticles in HeLa cells. The results suggest that HFR bioconjugate is a promising carrier for targeted delivery of hydrophobic PDT agents and as a potential nanocarrier for dual chemo-and photodynamic therapies.

Acknowledgements

This work was supported by a grant from the Fundamental R&D Program for Core Technology of Materials funded by the Ministry of Knowledge Economy and by Basic Science Research Program through the National Research Foundation of Korea (NRF) funded by the Ministry of Education, Science and Technology (2012005029). We also acknowledge the financial support of the Korea Ministry of Education, Science and Technology through Strategic Research (2011-0028726).

References

Bae, B.-C., & Na, K. (2010). Self-quenching polysaccharide-based nanogels of pullulan/folate-photosensitizer conjugates for photodynamic therapy. *Biomaterials*, *31*, 6325–6335.

Canal, F., Vicent, M. J., Pasut, G., & Schiavon, O. (2010). Relevance of folic acid/polymer ratio in targeted PEG-epirubicin conjugates. *Journal of Controlled Release*, *146*, 388–399.

Cho, K., Wang, X., Nie, S., Chen, Z., & Shin, D. M. (2008). Therapeutic nanoparticles for drug delivery in cancer. *Clinical Cancer Research*, *14*, 1310–1316.

Dolmans, D. E., Fukumura, D., & Jain, R. K. (2003). Photodynamic therapy for cancer. *Nature Review Cancer*, *3*, 380–387.

Duncan, R. (2003). The dawning era of polymer therapeutics. *Nature Reviews Drug Discovery*, *2*, 347–360.

Fernandez, J. M., Bilgin, M. D., & Grossweiner, L. I. (1997). Singlet oxygen generation by photodynamic agents. *Journal of Photochemistry and Photobiology B*, *37*, 131–140.

Fingar, V. H., Kik, P. K., Haydon, P. S., Cerrito, P. B., Tseng, M., Abang, E., et al. (1999). Analysis of acute vascular damage after photodynamic therapy using benzoporphyrin derivative (BPD). *British Journal of Cancer*, *79*, 1702–1708.

Gao, F. P., Zhang, H. Z., Liu, L. R., Wang, Y. S., Jiang, Q., Yang, X. D., et al. (2008). Preparation and physicochemical characteristics of self-assembled nanoparticles of deoxycholic acid modified-carboxylmethyl curdlan conjugates. *Carbohydrate Polymers*, *71*, 606–613.

Guo, M., Que, C., Wang, C., Liu, X., Yan, H., & Liu, K. (2011). Multifunctional superparamagnetic nanocarrier with folate-mediated and pH-responsive targeting properties for anticancer drug delivery. *Biomaterials*, *32*, 185–194.

Hajri, A., Wack, S., Meyer, C., Smith, M. K., Leberquier, C., Kedinger, M., et al. (2002). In vitro and in vivo efficacy of photofrin and pheophorbide a, a bacteriochlorin, in photodynamic therapy of colonic cancer cells. *Photochemistry and Photobiology*, *75*, 140–148.

Hoebeke, M., & Damoiseau, X. (2002). Determination of the singlet oxygen quantum yield of bacteriochlorin a: A comparative study in phosphate buffer and aqueous dispersion of dimiristoyl-L-alpha-phosphatidylcholine liposomes. *Photochemical Photobiological Sciences*, *1*, 283–287.

Hou, L., Fan, Y., Yao, J., Zhou, J., Li, C., Fang, Z., et al. (2011). Low molecular weight heparin-all-trans-retinoic acid conjugate as a drug carrier for combination cancer chemotherapy of paclitaxel and all-trans-retinoic acid. *Carbohydrate Polymers*, *86*, 1157–1166.

Lee, B. S., Park, K., Park, S., Kim, G. C., Kim, H. J., Lee, S., et al. (2010). Tumor targeting efficiency of bare nanoparticles does not mean the efficacy of loaded anticancer drugs: Importance of radionuclide imaging for optimization of highly selective tumor targeting polymeric nanoparticles with or without drug. *Journal of Controlled Release*, *147*, 253–260.

Lee, S. J., Park, K., Oh, Y.-K., Kwon, S.-H., Her, S., Kim, I.-S., et al. (2009). Tumor specificity and therapeutic efficacy of photosensitizer-encapsulated glycol chitosan-based nanoparticles in tumor-bearing mice. *Biomaterials*, *30*, 2929–2939.

Li, C., & Wallace, S. (2008). Polymer-drug conjugates: Recent development in clinical oncology. *Advanced Drug Delivery Reviews*, *60*, 886–898.

Li, L., Bae, B.-C., Tran, T. H., Yoon, K. H., Na, K., & Huh, K. M. (2011). Self-quenchable biofunctional nanoparticles of heparin-folate-photosensitizer conjugates for photodynamic therapy. *Carbohydrate Polymers*, *86*, 708–715.

Li, L., Moon, H. T., Heo, Y. J., Choi, Y., Tran, T. H., Lee, Y.-k., et al. (2011). Heparin-based self-assembled nanoparticles for photodynamic therapy. *Macromolecular Research*, *19*, 487–494.

Li, Y., Qi, X. R., Maitani, Y., & Nagai, T. (2009). PEG–PLA diblock copolymer micelle-like nanoparticles as all-trans-retinoic acid carrier: In vitro and in vivo characterization. *Nanotechnology*, *20*, 1–10.

Oh, I.-H., Cho, K. J., Tran, T. H., Huh, K. M., & Lee, Y.-k. (2012). Biofunctional nanoparticle formation and folate-targeted antitumor effect of heparin-retinoic acid conjugates. *Macromolecular Research*, *20*, 520–527.

Roslaniec, M., Weitman, H., Freeman, D., Mazur, Y., & Ehrenberg, B. (2000). Liposome binding constants and singlet oxygen quantum yields of hypericin, tetrahydroxy helianthrone and their derivatives: Studies in organic solutions and in liposomes. *Journal of Photochemistry and Photobiology B*, *57*, 149–158.

Sasisekharan, R., Shriver, Z., Venkataraman, G., & Narayanasami, U. (2002). Roles of heparan-sulfate glycosaminoglycans in cancer. *Nature Review Cancer*, *2*, 521–528.

Scomparin, A., Salmaso, S., Bersani, S., Fainaro, R. S., & Caliceti, P. (2011). Novel folated and non-folated pullulan bioconjugates for anticancer drug delivery. *European Journal of Pharmaceutical Sciences*, *42*, 547–558.

Wang, X., Li, J., Wang, Y., Cho, K. J., Kim, G., Gjyrezi, A., et al. (2009). HFT-T, a targeting nanoparticles, enhances specific delivery of pactitaxel to folate receptor-positive tumors. *ACS Nano*, *3*, 3165–3174.

Wang, Y., Wang, Y., Xiang, J., & Yao, K. (2010). Target-specific cellular uptake of taxol-loaded heparin-PEG-folate nanoparticles. *Biomacromolecules*, *11*, 3531–3538.